Renewable Energy 36 (2011) 1734–1740

Contents lists available at ScienceDirect

Renewable Energy

journal homepage: www.elsevier.com/locate/renene

An extension of BEM method applied to horizontal-axis wind turbine design

Jerson Rogério Pinheiro Vaz [a,*], João Tavares Pinho [b], André Luiz Amarante Mesquita [a]

[a] Universidade Federal do Pará - Faculdade de Engenharia Mecânica, Av. Augusto Correa, s/n - Belem, Pará 66075-900, Brazil
[b] Universidade Federal do Pará - Faculdade de Engenharia Elétrica, Av. Augusto Correa, s/n - Belém, Pará 66075-900, Brazil

ARTICLE INFO

Article history:
Received 6 July 2010
Accepted 11 November 2010
Available online 8 January 2011

Keywords:
Wind power
Wind turbine
BEM method
Glauert's model

ABSTRACT

A mathematical model is presented in this work, based on the Blade Element Momentum (BEM) theory for the horizontal-axis wind turbine design, taking into account the influence of the wake on the rotor plane in the general form. This influence is considered when the tip-speed-ratio is small, justifying the development of formulations that predict the effects of the wake on the rotor plane. The proposed mathematical model in this work is an extension of the BEM method, using the Glauert's model modified for the wind turbine design.

1. Introduction

The study of mathematical models applied to wind turbine design in recent years, principally in electrical energy generation, has become significant due to the increasing use of renewable energy sources with low environmental impact. Such methods are generally based on the Blade Element Momentum (BEM) Theory [2,4–6,16], which considers that the blade can be analyzed as a number of independent streamtubes, the spanwise flow is negligible, the flow is considered axisymetric, and usually the cascade effect is not taken into account. In each streamtube, the induced velocity is calculated by performing the conservation of the momentum, and the aerodynamic forces are found through two-dimensional airfoil data available in literature. In this classical model the induction factor in the wake is twice those on the rotor plane, ignoring the most general form to the influence of the wake. However, this is valid for fast rotor, where the tip-speed-ratio X is greater than 2. For the region of slower operation of the rotor, the model fails to provide reliable values, with respect to its performance. Thus, this paper shows an alternative mathematical scheme for the wind turbine design, which considers the influence of the wake in its most general form, correcting the high values of the induction factor on the rotor plane through a modification of the empirical relationship shown in Ref. [3].

The results from the BEM method are greatly dependent on the precision of the lift and drag coefficients. Generally, during an operational period of a wind turbine, due to the variations in the wind speed, the angle of attack can reach high values, and, for this condition (post-stall region), the aerodynamic data is not available. The available airfoil data is often limited to the range of angle of attack, as in Ref. [1]. When the rotor blades operate in the post-stall region, the BEM method underestimates the evaluated rotor power when compared to the experiments [13]. For the post-stall phenomenon, this work uses the mathematical model shown in [15] in which the values of lift and drag coefficients are extrapolated for angles of attack up to 90°. For the correction of the finite number of blades, it uses the Prandtl's tip-loss factor [7]. Finally, the results obtained using the proposed model are displayed and compared to theoretical and experimental data found in the literature.

The present work is an extension of the method presented in Ref. [11] and shows the development of the system's equations of the proposed model that is valid for the whole extension of the tip-speed-ratio range.

2. The mathematical model

A flow model that considers the complete angular momentum equations for fluid rotation on the wake was presented in Ref. [8] and applied in Ref. [3] in the study of propulsion, and later modified in Ref. [17] for the case of wind turbine design, where the induction factor caused by the wake is twice the induction factor on the rotor plane. Fig. 1 shows a scheme of the flow in a tube of currents [2].

The induced speeds u and u_1 in the rotor plane and the wake, respectively, are:

* Corresponding author. Tel.: +55 91 8179 5591.
E-mail address: jerson@ufpa.br (J.R.P. Vaz).

0960-1481
doi:10.1016/j.renene.2010.11.018

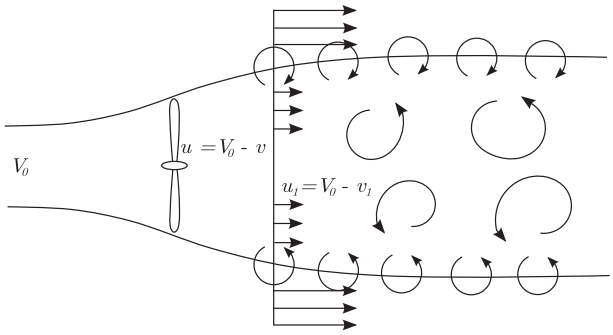

Fig. 1. Simplified scheme of speeds on a wind turbine [6].

$$\begin{cases} V_0 - v = u \equiv (1-a)V_0 \\ V_0 - v_1 = u_1 \equiv (1-b)V_0 \end{cases} \tag{1}$$

V_0 is the speed of undisturbed flow, a and b are the axial induction factors on the rotor plane and the wake, respectively, and defined by

$$a = \frac{V_0 - u}{V_0} \tag{2}$$

$$b = \frac{V_0 - u_1}{V_0} \tag{3}$$

Considering the hypothesis of the BEM method described previously, by applying the forces balance developed over a rotor blade section airfoil (see Fig. 2), and momentum, moment of momentum and mass conservation principle on an individual streamtube, the annulus flow equations are obtained as follows [4,5,17]:

$$a = \frac{b}{2}\left[1 - \frac{b^2(1-a)}{4X^2(b-a)}\right] \tag{4}$$

Where X is the tip-speed-ratio, defined by

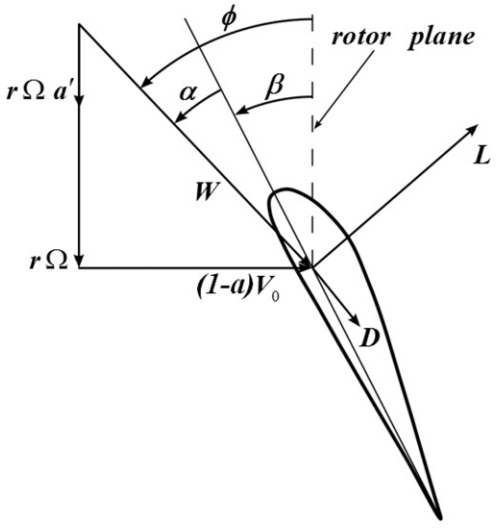

Fig. 2. Velocity diagram for a rotor blade section.

$$X = \frac{R\Omega}{V_0} \tag{5}$$

R is the rotor radius and Ω is the rotor angular velocity

Eq. (4) represents the most general relationship between a and b. To obtain this equation, it was assumed that $r^2\omega$ is constant, i.e., the rotor wake is an irrotational vortex, which has infinite velocities at the center of rotation. The Glauert's theory therefore predicts velocities which exceed the rotational speed of the blades close to the center of rotation. Due to this fact, Ref. [17] suggests a different procedure, substituting the irrotational vortex wake by a Rankine vortex wake. Although it is true that infinite velocities cannot exist, it is not clear why the wake rotational velocity cannot exceed that of the rotor. For this reason, [11], use the Glauert's scheme, which avoids the problem of the infinite velocities close to the rotation center, interrupting the integration of the equations in the radial position, where the wake angular velocity, ω, is equal to the rotor angular velocity, Ω. The present work consider the Eq. (4), but established the hypothesis that

$$\frac{a'}{a} = \frac{b'}{b} \tag{6}$$

$$a' = \frac{\omega}{\Omega} \tag{7}$$

$$b' = \frac{\omega_1}{\Omega} \tag{8}$$

where a' and b' are, respectively, the tangential induction factor at the rotor and the tangential induction factor at the rotor wake, and ω_1 is the flow angular velocity at the rotor wake.

The present work assumes that the induction factor b' has a similar relationship with a', which leads to a more general form than that one proposed by Mesquita and Alves [11], i.e.,

$$a' = \frac{b'}{2}\left[1 - \frac{b'^2(1-a')}{4X^2(b\prime - a\prime)}\right] \tag{9}$$

To solve the Eqs. (4) and (9), Newton's method is used, in which for each value calculated, there are 3° polynomial functions, given by

$$\Phi(b) = \frac{b}{2}\left[1 - \frac{b^2(1-a)}{4X^2(b-a)}\right] - a \tag{10}$$

$$\Gamma(b') = \frac{b'}{2}\left[1 - \frac{b'2(1-a')}{4X^2(b'-a')}\right] - a\prime \tag{11}$$

The iterative solution is obtained by Eqs. (12) and (13). In this case, a good approximation to begin the iterative process corresponds to $b = 2a$ and $b' = 2a'$.

$$b_i = b_{i-1} - \frac{\Phi(b_{i-1})}{\frac{d\Phi}{db}(b_{i-1})} \tag{12}$$

$$b'_i = b'_{i-1} - \frac{\Phi(b'_{i-1})}{\frac{d\Phi}{db'}(b'_{i-1})} \tag{13}$$

The use of Newton's method consists in always getting the lowest real value to calculate $b \in R$ and $b' \in R$, since the variation of induction factors in the wake is entirely non-linear regarding the induction factors on the rotor plane.

2.1. The correction for the Glauert's model

The Prandlt tip-loss model is the most accepted correction employed and is usually taken as corresponding to a model of the flow for a finite number of blades. Strip theory calculations made with the Prandtl model show good agreement with calculation made through free wake vortex theory and with test data [16]. A tip-loss factor F was introduced, which modifies the power output for the reduced circulation and blade unloading by tip-vortex shedding. This factor is defined by the ratio between the bound circulation of all the blades and the circulation of a rotor with infinite number of blades. It is given by

$$F = \frac{2}{\pi}\cos^{-1}[\exp(-f)] \tag{14}$$

$$f = \frac{B}{2}\frac{R-r}{r\sin\phi}, \text{ for the tip side} \tag{15}$$

$$f = \frac{B}{2}\frac{r-r_{\text{hub}}}{r_{\text{hub}}\sin\phi}, \text{ for the hub side} \tag{16}$$

Appling this correlation for the trust coefficient result in

$$C_T = \begin{cases} 4a(1-a)F; & a \le \frac{1}{3} \\ 4a\left[1-\frac{a}{2}(5-3a)\right]F; & a > \frac{1}{3} \end{cases} \tag{17}$$

a correction in Eq. (17) was developed, in order to consider the most general case to calculate the induction factor on the plane of the rotor, where the thrust coefficient is dependent on the induction factor in the wake. Thus, it assumes the following modifications:

$$C_T = \begin{cases} 2b(1-a)F; & a \le \frac{1}{3} \\ 2b\left[1-\frac{a}{2}(5-3a)\right]F; & a > \frac{1}{3} \end{cases} \tag{18}$$

The behavior of trust coefficient C_T as function of a is shown in Fig. 3, where an increase of C_T occurs for values of $X = (1.0, 1.5, 2.0)$, which is predicted by the relationship between b and a, where b assumes values greater than twice a, resulting in an increase of values of C_T for a around 0.5, since C_T is directly proportional to b.

The proposed scheme, using the most general form for the axial induction factor, converges to the classical BEM method, both with and without the correction of Ref. [3], where X is greater than 2, see Fig. 3. Fig. 4 compares the results with experimental data, obtained from Ref. [12], for $X = 4$, showing good agreement.

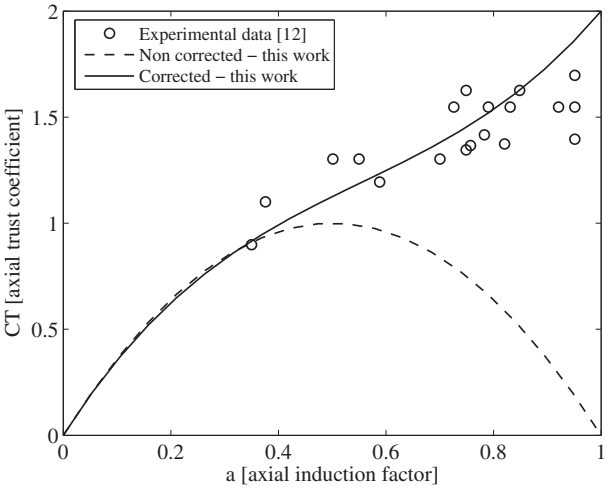

Fig. 4. Comparison between proposed model and experimental data for $X = 4$.

The model has good numerical stability even for values of $X < 2$ (see Fig. 5).

Eq. (18) shows that for $a > 1/3$ the thrust coefficient is corrected to values of b. Since the C_T in the rotor plane is

$$C_T = (1-a)^2\frac{\sigma C_n}{\sin^2\phi} \tag{19}$$

given in Ref. [6], where

$$\sigma = \frac{cB}{2\pi r} \tag{20}$$

$$C_n = C_L\cos\phi + C_D\sin\phi \tag{21}$$

Equating (18) and (19)

$$a = \begin{cases} 1-\frac{2bF\sin^2\phi}{\sigma C_n}; & a \le \frac{1}{3} \\ \frac{8-5k-\sqrt{k(32-23k)}}{2(4-3k)}; & a > \frac{1}{3} \end{cases} \tag{22}$$

with

$$k = \frac{2bF\sin^2\phi}{\sigma C_n} \tag{23}$$

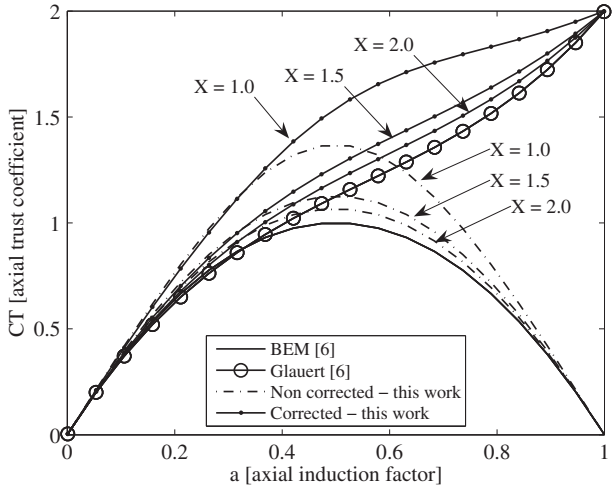

Fig. 3. Solutions for the proposed model, BEM and Glauert's methods for some values of X.

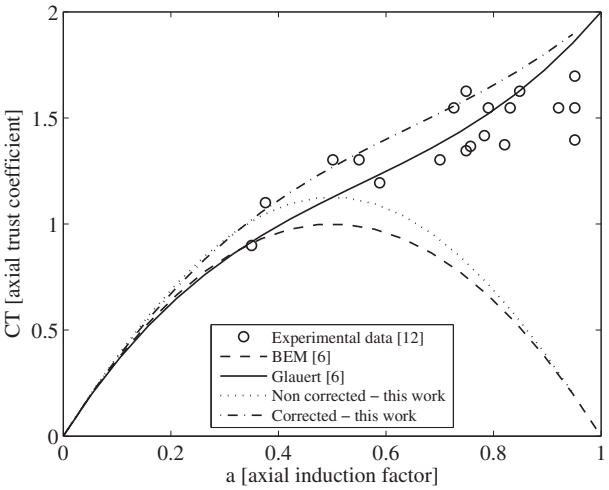

Fig. 5. Results for $X = 1.5$.

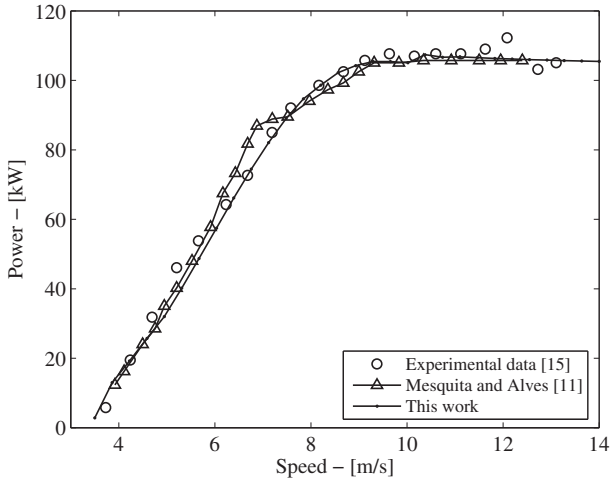

Fig. 6. Experimental and theoretical power for the rotor MOD 0.

where B is the number of blades, c is the local chord, r is the local radius, C_L and C_D are the lift and drag coefficients, respectively, ϕ is the angle of flow given by equation

$$\phi = \tan^{-1}\left[\frac{V_0(1-a)}{\Omega r(1+a\prime)}\right] \tag{24}$$

For the calculation of a'.

$$a\prime = \frac{2b\prime F\sin\phi\cos\phi}{\sigma C_t} - 1 \tag{25}$$

Eq. (25) can be found in the work of Ref. [11], where $C_t = C_L\sin\phi - C_D\cos\phi$ is the tangential force coefficient.

The iterative procedure for the calculation of induction factors, considers known parameters r, $c(r)$, $\beta(r)$, $C_L(\alpha)$, $C_D(\alpha)$ and V_0 given as follows:

(i) Attribute initial values for a and a'. In this work $a = 1/3$ and $a' = 0.001$;
(ii) Compute b and b' through Eqs. (12) and (13);
(iii) Compute ϕ through Eq. (24);
(iv) Obtain C_L and C_D of $\alpha = \phi - \beta$, where α is angle of attack and β the angle of twist;
(v) Compute a and a', applying Newton's method in Eqs. (22) and (25), making

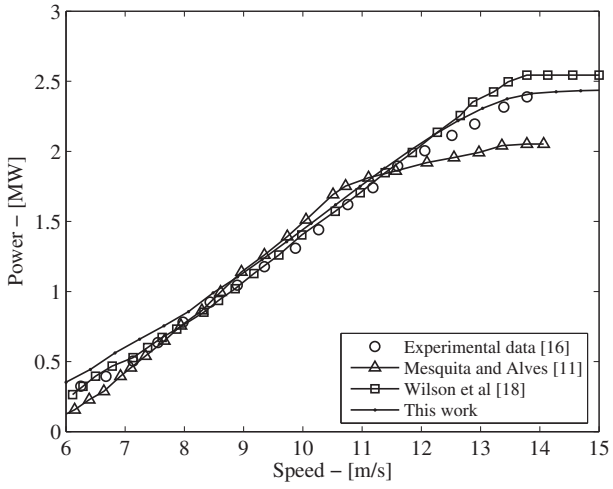

Fig. 7. Experimental and theoretical power for the rotor MOD2.

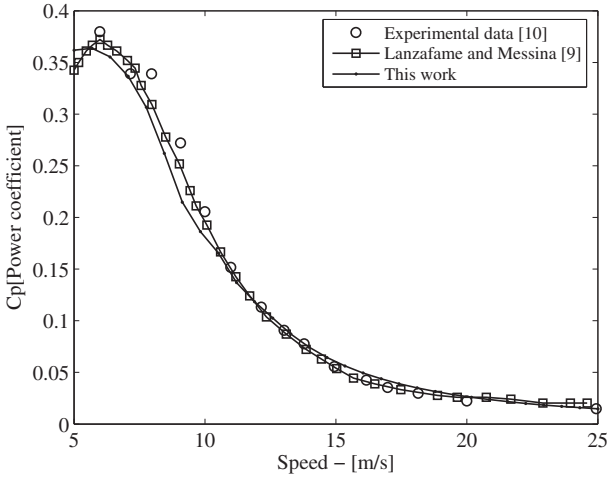

Fig. 8. Experimental comparison for the rotor UAE Phase IV.

$$\Psi(a) = -a + 1 - \frac{2bF\sin^2\phi}{\sigma C_n} \tag{26}$$

$$\Pi(a') = -a\prime - 1 + \frac{2b\prime F\sin\phi\cos\phi}{\sigma C_t} \tag{27}$$

Since the induction factors in the wake depend on the induction factors on the rotor plane, $b = b(a)$ and $b\prime = b\prime(a')$, thus

$$a_i = a_{i-1} - \frac{\Psi(a_{i-1})}{\frac{d\Psi}{da}(a_{i-1})} \tag{28}$$

$$a'_i = a'_{i-1} - \frac{\Pi(a'_{i-1})}{\frac{d\Pi}{da'}\left(a'_{i-1}\right)} \tag{29}$$

(vi) Apply the Glauert's model modified through Eq. (22);

(vii) Verify the convergence for a and a'. In this work the tolerance is considered 10^{-3}. If there is no convergence, the procedure is restarted from step (ii).

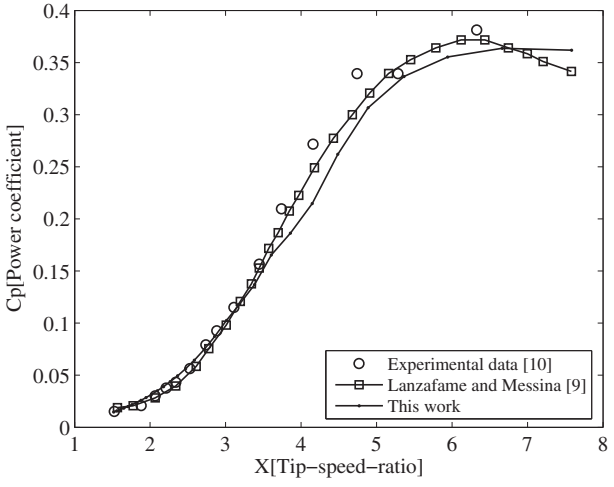

Fig. 9. Power coefficient in relation to tip-speed-ratio X and experimental comparison for the rotor UAE Phase IV.

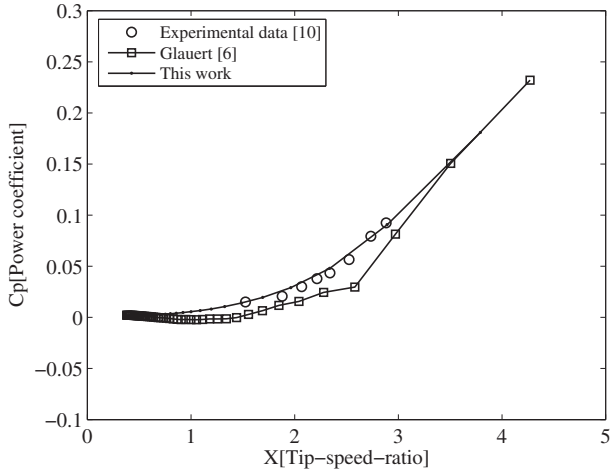

Fig. 10. Effects of the model at low tip-speed-ratio in the case of Phase IV UAE Turbine.

The power coefficient Cp, as given in Ref. [11], is

$$Cp = \frac{4}{X^2}\int_0^X (1 - aF)Fb'x^3 \mathrm{d}x \tag{30}$$

3. Correction for the stall using the Viterna and Corrigan model

Viterna and Corrigan [15], proposed an empirical model to modify the aerodynamic parameters of lift and drag in the stall development regime, in order to predict accurately the behavior of a wind turbine. Thus, when the angle of attack is equal or greater to that in which the separation phenomenon initiates, the model predicts the following figures for the lift and drag coefficients:

$\alpha \geq \alpha_{\text{separation}}$:

$$C_l = \frac{C_{d,\,\max}}{2}\sin 2\alpha + K_l\frac{\cos^2\alpha}{\sin\alpha} \tag{31}$$

$$C_d = C_{d,\,\max}\sin^2\alpha + K_d\cos\alpha \tag{32}$$

$$K_l = \left(C_{l,s} - C_{d,\,\max}\sin\alpha_s\cos\alpha_s\right)\frac{\sin\alpha_s}{\cos^2\alpha_s} \tag{33}$$

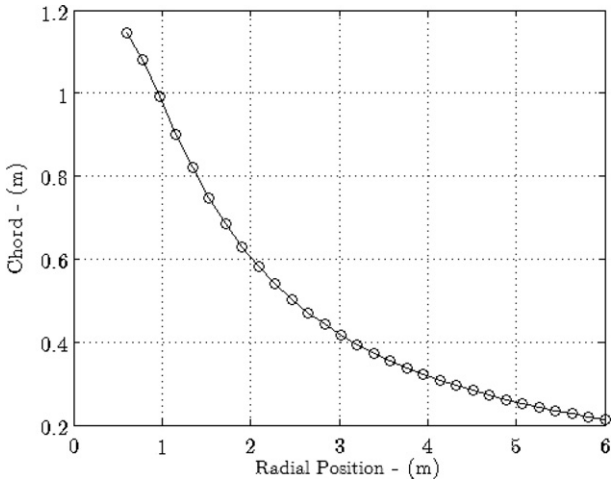

Fig. 11. Chord distribution.

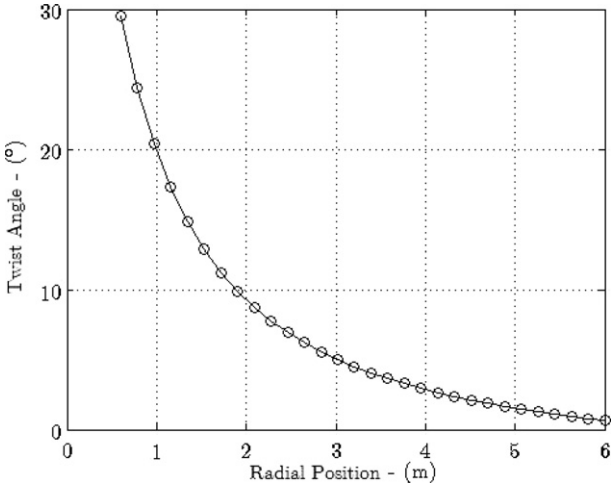

Fig. 12. Twist angle distribution of the wind rotor.

$$K_d = \frac{C_{d,s} - C_{d,\max}\sin^2\alpha_s}{\cos\alpha_s} \tag{34}$$

$$\mu \leq 50 : C_{d,\,\max} = 1.11 + 0.018\mu \tag{35}$$

$$\mu > 50 : C_{d,\,\max} = 2.01 \tag{36}$$

where μ is the aspect ratio, defined by

$$\mu = \frac{R - r_{\text{hub}}}{c(r)} \tag{37}$$

and $C_{d,\,\max}$ is the maximum drag coefficient on the completely separate regime.

4. Results

The results are validated by comparing the performance of the proposed model with other models. The rotors used in the comparison are MOD 0 and MOD 2, whose experimental data were collected by NASA Lewis Research Center, Phase VI and the UAE, with experiments carried out by NREL in the wind tunnel at NASA-ASME [15,16].

The turbine MOD 0 corresponds to a 2-blade rotor, rated power at 100 kW. The used profile is the NACA series 23000, constant rotation of 27 rpm, pitch angle of 0°. The chord distribution is 1.96 m for $r/R = 0.234$, varying linearly up to 0.67 m for $r/R = 1$, the

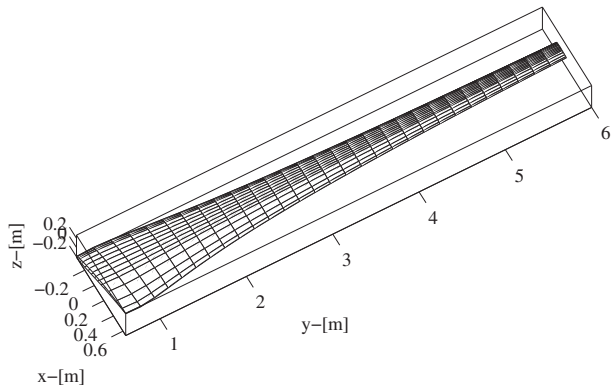

Fig. 13. Blade obtained from chord and twist angle distributions shown in Figs. 11 and 12.

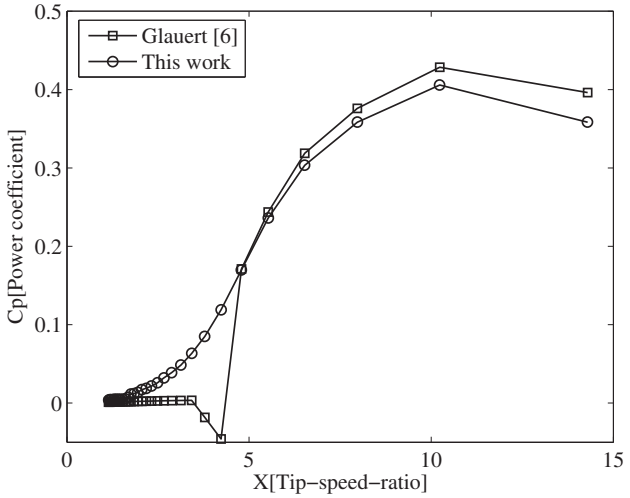

Fig. 14. Power coefficient in relation to tip-speed-ratio for rotational speed of 91 rpm.

rotor diameter is 38 m and the hub diameter is 7.84 m [15]. Fig. 6 shows the behavior of the output power generated by this model, which presents a better agreement with the experimental results.

The turbine MOD 2 corresponds to a 2-blade rotor, rated power at 2.5 MW. The used profile is the NACA series 23024, constant rotational speed of 17.5 rpm, twist angle variable linearly from the $-5°$ to $-2°$ from on 70% of radius. The chord is 3.45 m to $r/R = 0.297$, varying linearly up to 1.43 m for $r/R = 1$, the rotor diameter is 91.4 m and the hub diameter is 18 m [16]. Fig. 7 compares the result obtained for speeds ranging from 6 to 15 m/s, where the power curve shows good agreement with the results experimentally obtained, and improved when compared with Refs. [18] and [11].

For the UAE Phase IV turbine, there are 2 blades, with twist and chord distributions variables along the blade and a diameter of 10.029 m. The airfoil is the S809, constant throughout the rotor, the pitch angle is 3° and the rotation is kept constant at 72 rpm [6,10].

The result is compared with experimental data, as well as those obtained in Ref. [9]. In Figs. 8 and 9 it can be observed that the proposed model also shows good agreement.

Experimental data for low tip-speed-ratio are very difficult in the literature. However an assessment of the effects of the proposed model at low tip-speed-ratio is shown in Fig. 10, where the model is compared with the classical Glauert model [6] and

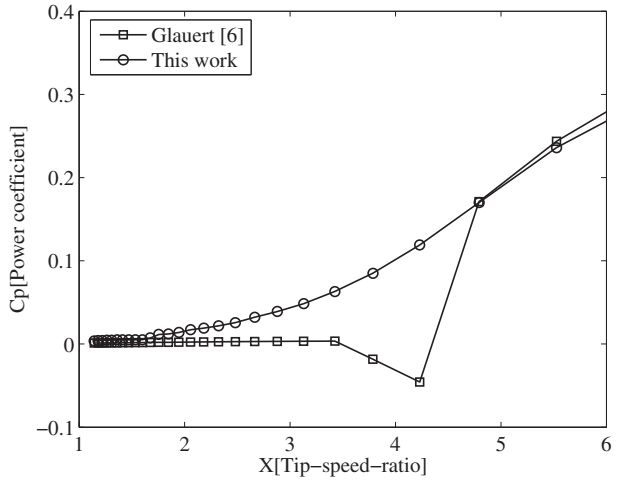

Fig. 15. Effects of the model at low tip-speed-ratio.

experimental data obtained for the Phase IV UAE turbine [10] in the region of operation where the tip-speed-ratio is between 1.5 and 3.2. Note that the model shows good agreement with experimental data, which does not occur with the classical model of Glauert [6].

Figs. 11 and 12 show the chord and twist angle distribution along the radius for a small rotor, designed using the numerical code implemented in this work. The aerodynamic parameters for determining the blade shown in Fig. 13 were obtained using the profile A18 [14].

In this case, it is observed from Fig. 14, that for values of X close to 2 the BEM model with the Glauert correction fails, while the proposed model presents continuity even though the rotor experiences low angular speed.

For this specific design, where the operation conditions bring the turbine to a zone of low X the proposed model is adequate to evaluate de power generation. It is observed on Fig. 15 that for low values of X, the BEM model with the Glauert correction fails.

5. Conclusions

An improved approach for performance prediction of horizontal-axis wind turbine design using the BEM theory and some empirical corrections was presented. The correction was employed in order to consider the tip-loss, cascade, post-stall and turbulent wake effects. The new model represents an extension of the model developed in Ref. [11], which extends the validity of the usual strip theory models for the whole extension of the tip-speed-ratio region. The equations presented express the axial induction factor at the rotor wake.

The mathematical model presented in this paper introduces an alternative tool for the wind turbine design, specially for slow rotors, once it is predicted in its main structure the most general equation that relates the induction factors in the rotor plane and the wake, based on the Glauert's theory and BEM model, that were modified here to predict the conditions set by Eqs. (4) and (9).

The comparisons carried out show that the model has good performance when compared to other models in the literature and that can be used in wind turbine design.

Acknowledgments

The present work was developed by Grupo de Estudos e Desenvolvimento de Alternativas Energéticas - GEDAE, member of Instituto Nacional de Ciência e Tecnologia de Energias Renováveis e Eficiência Energética da Amazônia - INCT - EREEA. The authors would like to thank Conselho Nacional de Desenvolvimento Científico e Tecnológico - CNPq for financial support.

References

[1] Abbott IH, Von Doenhoff AE. Theory of wing sections. Including a summary of airfoil data. New York: Dover; 1959.
[2] Eggleston DM, Stoddard FS. Wind turbine engineering design. New York: Van Nostrand Reinhold Company; 1987.
[3] Glauert H. The elements of airfoil and airscrew theory. New York: Cambridge University Press; 1926.
[4] Glauert H. Airplanes propellers. In: Durand WF, editor. Aerodynamic theory. Berlin: Julius Springer; 1935a. p. 191–5.
[5] Glauert H. Windmills and fans. In: Durand WF, editor. Aerodynamic theory. Berlin: Julius Springer; 1935b. p. 338–41.
[6] Hansen AC, Butterfield CP. Aerodynamics of horizontal axis wind turbines. Annual Review of Fluid Mechanics 1993;25:115–49.
[7] Hibbs B, Radkey RL. Small wind energy conversion systems (swecs) rotor performance model comparison study; 1981. Tech. rep., Rockwell Int. Rocky Flats Plant, rFP-4074/13470/36331/81–0.
[8] Joukowski NE. Travaux du bureau des calculs et essais aeronautiques de l'ecole superièure technique de moscou; 1918.

[9] Lanzafame R, Messina M. Fluid dynamics wind turbine design: Critical analysis, optimization and application of bem theory. Renewable Energy 2007; 32(14):2291–305.
[10] Lindenburg C. Investigation into rotor blade aerodynamics; 2003. ecn-c-03–025.
[11] Mesquita ALA, Alves A. An improved approach for performance prediction of HAWT using the strip theory. Wind Engineering 2000;24(6):417–30.
[12] Moriarty PJ, Hansen AC. Aerodyn theory manual. Tech. Rep. NREL/TP-500–36881. Golden, CO: National Renewable Energy Laboratory; 2005.
[13] Musial WD, Butterfield CP, Jenks MD. A comparison of two-and three-dimensional S809 airfoil properties for rough and smooth HAWT (Horizontal-Axis Wind Tunnel) rotor operation. In: Proceedings of the 9th ASME wind energy; Feb 1990. p. 14–7. New Orleans, USA.
[14] Selig MS, Guglielmo JJ, Broeren AP, Giguère P. Summary of low-speed airfoil data. Virginia Beach, VA, USA: SoarTech Publications; 1995.
[15] Viterna LA, Corrigan RD. Fixed pitch rotor performance of large horizontal axis wind turbines. Tech. rep. Cleveland, Ohio, USA: Glenn Research Center; 1982.
[16] Wilson RE. Aerodynamic behavior of wind turbines. In: Spera DA, editor. Wind turbine technology. New York, USA: ASME Press; 1994.
[17] Wilson RE, Lissaman PBS. Applied aerodynamics of wind power machines. Tech. Rep NSF-RA-N-74-113. Oregon State University; 1974.
[18] Wilson RE, Lissaman PBS, Walker SN. Aerodynamic performance of wind turbines. Tech. Rep. ERDA/NSF/04014-76/1. Washington, DC, USA: Department of Energy; 1976.